MESOSPHERE DYNAMICS WITH GRAVITY WAVE FORCING: 2, PLANETARY WAVES

H. G. Mayr[1], J. G. Mengel[2], K. L. Chan[3], and H. S. Porter[4]

[1]NASA Goddard Space Flight Center, Greenbelt, MD

[2]SM&A Corporation, Vienna, VA

[3]Hong Kong University of Science and Technology, Hong Kong, China.

[4]Furman University, Greenville, SC

Prepared for Publication

in

Journal of Atmospheric and Solar Terrestrial Physics

September 2000

ABSTRACT: We present results from a non-linear, 3D, time dependent numerical spectral model (NSM), which extends from the ground up into the thermosphere and incorporates Hines' Doppler Spread Parameterization for small-scale gravity waves (GW). Our focal point is the mesosphere where wave interactions are playing a dominant role. We discuss planetary waves in the present paper (Part II) and diurnal and semi-diurnal tides in the companion paper (Part I). Without external time dependent energy or momentum sources, planetary waves (PW) are generated in the model for zonal wavenumbers 1 to 4, which have amplitudes in the mesosphere above 50 km as large as 30 m/s and periods between 2 and 50 days. The waves are generated primarily during solstice conditions, which indicates that the baroclinic instability (associated with the GW driven reversal in the latitudinal temperature gradient) is playing an important role. Results from a numerical experiment show that GW's are also involved directly in generating the PW's. For the zonal wavenumber m = 1, the predominant wave periods in summer are around 4 days and in winter between 3 and 10 days. For m = 2, the periods are in summer and winter close to 2.5 and 3.5 days respectively. For m = 3, 4 the predominant wave periods are in both seasons close to 2 days. The latter waves have the characteristics of Rossby gravity waves, with large meridional winds at equatorial latitudes. A common feature of the PW's (m = 1 to 4) generated in summer and winter is that their vertical wavelengths throughout the mesosphere are large, which indicates that the waves are not propagating freely but are generated throughout the region. Another common feature is that the PW's propagate preferentially westward in summer and eastward in winter, being launched from the westward and eastward zonal winds that prevail respectively in summer and winter at altitudes below 80 km. During spring and fall, for m = 1 and 2, eastward propagating, long period PW's are generated that are launched from the smaller eastward zonal winds that prevail in these seasons. As shown in Part I, the PW's generated in the model produce large amplitude modulations of the diurnal tides at altitudes above 80 km and contribute to their seasonal variations.

1. Introduction

Planetary waves (Rossby waves and Kelvin waves) are large-scale oscillations of the atmosphere under the influence of the Coriolis force. These waves are prominent features of the

troposphere and stratosphere, but have also been observed in the upper mesosphere. Ground-based measurements at heights between 80 and 100 km have detected oscillations with planetary wave periods (e.g., Muller and Nelson, 1978; Craig and Elford, 1981; Burks and Leovy, 1986; Tsuda et al., 1988; Phillips, 1989; Poole, 1990; Fraser et al., 1993; Clark et al., 1994; Fritts and Isler, 1994; Meek et al., 1996; Deng et al., 1997; Williams et al., 1999; Zhou et al., 2000), and planetary waves have been identified from the HRDI (Hays et al., 1993) and WINDII (Shepherd et al., 1993) measurements on the UARS spacecraft (e.g., Wu et al., 1993; Smith, 1996, 1997; Fritts et al., 1999; Wang et al., 2000). The theoretical treatments of planetary are reviewed by Volland (1988) and Forbes (1995).

Waves originating in the troposphere and near the ground, due to topographic forcing and tropical convection, are important for the dynamics of the stratosphere. At low latitudes, equatorially trapped Kelvin waves and Rossby gravity waves are involved in driving the Quasi-biennial Oscillation (QBO) and Semi-annual Oscillation. At mid and high latitudes, extra-tropical planetary waves affect significantly the seasonal variations in the global-scale zonal circulation and temperature distribution.

In the upper mesosphere, planetary waves with amplitudes as large as 100 m/s are observed, and there is evidence that they propagate into the thermosphere. Waves at these altitudes are not likely to have originated in the troposphere since they cannot propagate through the stratosphere and lower mesosphere without being dissipated. A significant portion of these waves must be excited in the mesosphere itself, and the dynamical conditions in this region are well suited for that. In a study conducted with a semi-spectral numerical model originally developed by Holton and Wehrbein (1981), Holton (1984) concluded that gravity waves originating in the troposphere are possibly a source for planetary waves in the mesosphere.

As Lindzen (1981) had shown and numerous modeling studies since, small-scale gravity waves that propagate up into the mesosphere cause the temperature variation to reverse against the pressure gradient, with the temperature decreasing across the globe from the winter hemisphere towards the summer hemisphere, as observed. The region is thus baroclinically unstable, and this can provide the energy to excite planetary waves as shown by Plumb (1983) and Pfister (1985). Plumb et al. (1986) also investigated how the 2-day planetary wave can influence the mesospheric circulation. The 2-day planetary wave in the mesosphere has been the subject of studies with the use of a middle atmosphere GCM (Norton and Thuburn, 1996, 1999).

It was shown there that for zonal wavenumbers m = 3 and 4 planetary waves are generated due to baroclinic instability as suggested by Plumb (1983) and that gravity wave drag is essential for that. Early results with our model that employed Rayleigh friction (Chan et al., 1994) to simulate the observed temperature reversal in the mesosphere produced a 4 day planetary wave for the zonal wavenumber m = 1. This wave was generated in the summer hemisphere near 80 km, and the baroclinic instability was identified as the cause.

In a companion paper (Part I), we discuss numerical results for the diurnal and semi-diurnal tides obtained from our model. In this paper, we discuss planetary waves. Alluding to Part I, we shall briefly discuss in Section II the properties of the numerical model and the approach taken in our analyses. In Section III, we describe the seasonal and height variations of the planetary waves that are generated in the model without external time dependent excitation source; the emphasis will be to assess the role played by gravity wave forcing. In Section IV, we summarize the results and present our conclusions.

II. Model and Analysis Approach

The organization of our model is illustrated in Figure 1 of Part I. The Numerical Spectral Model (NSM), introduced by Chan et al. (1994), is three dimensional, time-dependent and nonlinear. The NSM now incorporates the Doppler Spread Parameterization (DSP) for small-scale gravity waves (GW) developed by Hines (1994a, b), which provides the GW momentum source and related eddy diffusivity. Preliminary results from the 3-D version of the NSM have been discussed to describe the diurnal tides and equatorial oscillations (Mayr et al., 1998, 1999).

The NSM extends from the ground up into the thermosphere and computes the wind field and the perturbations of globally averaged temperature and density variations. For the zonal mean (m = 0), the solar UV heating above 15 km is taken from Strobel (1978), tropospheric heating is not accounted for. The diurnal tides (m = 1 and 2) are thermally excited by solar radiation absorbed in the water vapor layer near the ground and by ozone around 50 km [taken from Forbes and Garrett (1978)], and by UV and EUV radiation in the thermosphere. Planetary waves (PW) are not excited externally, either thermally or through a momentum source. Homogeneous boundary conditions are applied at the Earth's surface and upper boundary

the latitudinal temperature gradient across the globe that develops at altitudes above 50 km. As seen from Figure 1b, PW's are generated during winter and summer months. But their amplitudes are much smaller than those shown in Figure 1a. While the baroclinic instability is apparently involved in initiating the PW's, the GW momentum source is significantly amplifying them. When the GW source is turned off, the PW are also much weaker during the spring and fall seasons.

To provide a picture of the latitudinal and seasonal PW activity, we present in Figure 2 a contour plot of the zonal wind oscillations (computed with GW interaction) at 80 km for the month following June solstice. This shows that the wave amplitudes decrease from the polar region in summer towards the equator and across and then slightly increase again into the winter hemisphere, revealing a pattern consistent with that shown in Figure 1a. The waves in the summer hemisphere, at least initially, appear to propagate equatorwards; and there is some indication that this is also happening in the winter hemisphere.

A picture of the PW phase progression with altitude is presented in Figure 3, where we show contour plots of the zonal winds at northern polar latitudes for the summer month following June solstice. The large vertical wavelengths indicate that the PW are not freely propagating but are generated throughout the region, in part at least by the baroclinic instability. And the height variations of the wave patterns at other latitudes (not shown) lead to a similar conclusion.

To provide more details about the PW's generated in the model (with GW interaction), we present in Figure 4 segments of the zonal wind oscillations at northern mid latitudes and at 80 km for a period of 2 months following June (summer) and December (winter) solstices. For these periods, a running Fourier analysis was carried out to derive the peak spectra for the eastward and westward propagating wave components. The results show that during the summer months the waves propagate preferentially westward and the period for the peak amplitude is 4 days. In contrast, the waves tend to propagate preferentially eastward in winter and have periods covering a range from about 3 to 8 days.

Wavenumber m = 2: In Figure 5a we present the zonal wind oscillations for m = 2 computed with GW forcing. The seasonal variations of the PW's generated in the model at different altitudes are remarkably similar to those shown in Figure 1a. The growth in amplitude from 60 to 80 km is seen again, and long period waves appear in fall and late spring. Without GW source (Figure 5b), the PW's are also much weaker, like in Figure 1b.

Analogous to Figure 2, we present with Figure 6 a contour plot of the computed PW pattern at 80 km. But here, in contrast to Figure 2, the indication is that the waves are propagating towards higher latitudes. The waves also do not grow in amplitude towards the poles, simply due to the fact that the horizontal winds for $m \neq 1$ must vanish there. As shown in Figure 3 for $m = 1$, the height progression of the computed PW's in Figure 7 indicates that the waves are not propagating freely but are generated throughout the region.

The wave spectra presented in Figure 8 (analogous to Figure 4) again show that the computed PW's tend to propagate preferentially westward in summer and eastward in winter. But here the period of the dominant wave is close to 3 days in both seasons, only slightly longer in winter than in summer.

Wavenumber m = 3. In Figures 9a and 9b, we present the meridional wind oscillations for $m = 3$ at the equator computed with and without GW forcing. This shows PW being excited above 40 km, primarily during solstice condition, with amplitudes somewhat larger in summer than in winter. Throughout the year, the waves are virtually monochromatic, having a period close to 2 days at 80 km but distinctly longer at 60 km. As seen earlier, the waves are excited without GW forcing presumably due to baroclinic instability. And again, the GW's greatly amplify the PW's. In contrast to $m = 1, 2$, the PW's in Figure 9 do not reveal abatement at 100 km, which is partially understandable considering that viscous dissipation is relatively less effective for these waves having shorter oscillation periods.

For a short period following June solstice, we present in Figure 10 the latitudinal variations in the meridional wind oscillations at 80 km (computed with GW forcing). This shows again that the PW's are larger in the summer hemisphere than in winter. It also shows large meridional wind oscillations at the equator, which is characteristic of Rossby gravity waves. In the summer hemisphere these waves tend to propagate poleward. In the winter hemisphere at higher latitudes, in contrast, the pattern is distinctly different indicating that the PW's tend to propagate equatorward.

We present in Figure 10 for June solstice the height variations of computed PW's at 4° N. As discussed earlier for the lower wavenumbers, this shows again large vertical wavelengths indicating that the waves are not freely propagating but are generated throughout the region. Below 60 km, the waves are propagating down.

For a 2 months period following June solstice at mid latitudes and 80 km, we present the waves and wave spectra for the zonal winds in Figure 12. The predominant wave period is close to 2 days, and the PW again propagate preferentially westward in summer and eastward in winter.

A snapshot of the latitudinal variations of horizontal winds near June solstice are presented in Figure 13 and shows large meridional winds and vanishing zonal winds at the equator, characteristic of Rossby gravity waves. Although the wind velocities are significantly smaller in winter, the overall wave pattern there is similar to that in summer.

Wavenumber m = 4. In many ways, the waves generated for m = 4 show characteristics similar to those for m = 3. Analogous to Figure 8a, we present with Figure 14 the meridional wind oscillations computed with GW forcing. Waves are generated primarily around solstice. Without GW source the computed PW's (not shown) are again much weaker, which is consistent with the pattern seen in the earlier results.

The latitudinal variations in the PW's shown in Figure 15 again reveal larger amplitudes in summer than winter. In the summer hemisphere the waves tend to propagate poleward but the picture is not that clear in the winter hemisphere.

The height variations (not shown) again produce the picture of waves that are not propagating freely but are generated in the mesosphere. By comparison with Figure 10, one difference is that the waves are generated at higher altitudes.

Finally we present with Figure 16 the zonal winds and their spectra computed during summer and winter months at mid latitudes. These show that the wave periods in both seasons are close to 2 days and that the PW's again propagate westward in summer and eastward in winter.

IV. Summary and Conclusion

We have presented here a survey of the PW's that are generated in our global-scale Numerical Spectral Model (NSM) that employs Hines' Doppler Spread Parameterization for small-scale gravity waves (GW). Without external, time dependent energy or momentum sources, the model produces at altitudes above 50 km PW's for m = 1 to 4 with amplitudes near 30 m/s, which are generated internally due to dynamical interactions. As pointed out earlier, however, the PW amplitudes are smaller when the model computes self consistently with GW forcing the dynamical components m =

0 to 4. The results presented here are geared specifically to describe and understand the extent to which PW's are influenced directly by GW forcing.

In general, PW's appear in the model throughout the year and all over the globe in particular for m = 1, 2. Large PW's are generated preferentially around solstice, and the largest waves tend to occur in the summer hemisphere, which indicates that the baroclinic instability is involved in exciting them.

This baroclinic instability is caused by the reversal in the latitudinal temperature gradient for the zonal mean (m = 0) around solstice at altitudes above 60 km, and GW's are responsible for that (Lindzen, 1981). But GW's also affect the PW's directly. To demonstrate that, we carried out a numerical experiment in which the zonal mean temperature and wind fields (m = 0), computed self consistently with GW forcing, are applied in the model with and without GW forcing for m = 1 to 4. The results show that indeed PW's are excited preferentially during solstice conditions when the baroclinic instability comes into play. But without the direct GW forcing, the wave amplitudes are much smaller. In addition to the channel through the baroclinic instability, GW's are playing a major role directly in generating the PW's in the model.

The phase of the PW's progresses generally downwards. The vertical wavelengths, however, are large and indicate that the waves are not propagating freely but are excited throughout the mesosphere at altitudes above 50 km.

Our analysis of the PW's reveals relatively simple patterns seen in the predominant wave periods depending on the zonal wavenumber, and in the propagation directions depending on season. For m = 1, the dominant wave periods are close to 4 days in summer and between 2 and 8 days during winter months; for m = 2, the periods are close to 2.5 and 3.5 respectively in summer and winter; and for m = 3 and 4, the periods in both seasons are about 2 days. Irrespective of wavenumber, the waves propagate predominantly westward in summer and eastward in winter.

For m = 3 and 4, the westward propagating PW's in the summer hemisphere extend across the equator and represent Rossby gravity waves, characterized by their large meridional (and small zonal) winds at equatorial latitudes.

To provide an understanding of the above results it is instructive to look for mid latitudes at the propagation velocities, V, of the PW's. These are respectively for summer and winter (in m/s), V = 70, 47 (m = 1); 56, 40 (m = 2); 47, 47 (m = 3); 35, 35 (m = 4). The propagation velocities of the PW's produced in the model are close to zonal wind velocities in the summer and winter hemispheres

that are directed westward in summer and eastward in winter. The PW's are apparently generated as stationary oscillations, and their periodicities and propagation directions are largely determined by the flow medium in which they originate. This picture is consistent with the large vertical wavelengths of the PW's, which indicates, as pointed out earlier, that the waves are not propagating freely but are generated throughout the region.

Our interpretation may also explain why the PW's generated during spring and fall for m = 1 and 2 tend to have such large oscillation periods. During these seasons, the zonal winds in which the waves originate are much smaller than those during summer and winter months. The apparent propagation velocity (eastward presumably) is then also smaller, which translates into longer oscillation periods for a given zonal wavenumber.

As in the GCM simulations of Norton and Thuburn (1997, 1999), we are generating in our model mesospheric planetary waves without forcing from the lower atmosphere. The amplitudes from our model, however, are much smaller than those produced by Norton and Thuburn. Our numerical results confirm the theoretical analyses of Plumb (1983) and Pfister (1985), which led them to conclude that the baroclinic instability is involved in generating planetary waves in the mesosphere. Our results also show that gravity waves are involved directly – not only through the baroclinic instability. Based on a modeling study, Holton (1983) had suggested that upward propagating gravity waves would play such a role.

References

Allen, S. J., and S. A. Vincent, Gravity wave activity in the lower atmosphere: Seasonal and latitudinal variations, *J. Geophys. Res.*, **100**, 1327, 1995

Burks, D., and C. Leovy, Planetary waves near the mesospheric easterly jet, *Geophys. Res. Lett.*, **13**, No. 3, 193, 1986

Chan, K., L., H. G. Mayr, J. G. Mengel, and I. Harris, A spectral approach for studying middle and upper atmospheric phenomena, *J. Atmos. Terr. Phys.*, **56**, 1399, 1994

Clark, R. R., A. C. Current, A. H. Manson et al., Global properties of the 2-day wave from mesosphere lower-thermosphere radar observations, *J. Atmos. Terr. Phys.*, **56**, 1279, 1994

Craig, R. L., and W. G. Elford, Observations of the quasi 2-day wave near 90 km altitude at Adelaide (33° S), *J. Atmos. Terr. Phys.*, **43**, 1051, 1981

Deng, W., J. E. Salah, R. R. Clark et al., Coordinated global radar observations of tidal and planetary waves in the mesosphere and lower thermosphere during January 20-30, 1993, *J. Geophys. Res.*, **102**, 7307, 1997

Flaser, G. J., G. Hernadez, and R. W. Smith, "Eastward moving 2-4 day waves in the winter antarctic mesosphere, *Geophys. Res. Lett.*, **20**, 1547, 1993

Forbes, J. M., and H. B. Garrett, Thermal excitation of atmospheric tides due to insolation absorption by O_3 and H_2O, *Geophys. Res. Lett.*, **5**, 1013, 1978

Forbes, J. M., Tidal and planetary waves, *Geophysical Monograph* **87**, 67, 1995

Fritts, D. C., and J. R. Isler, Mean motion and tidal and 2-day structure and variability in the mesosphere and lower thermosphere, *J. Atmos. Sci.*, **51**, 2145, 1994

Fritts, D. C., J. R. Isler, R. S. Lieberman et al., Two-day wave structure and mean flow interactions observed by radar and High Resolution Doppler Imager, *J. Geophys. Res.*, **104**, 3953, 1999

Hays, P. B. et al. The high-resolution Doppler imager on the Upper Atmosphere Research Satellite, *J. Geophys. Res.*, **98**, 10,713, 1993

Hines, C. O., Doppler-spread parameterization of gravity-wave momentum deposition in the middle atmosphere, 1, Basic formulation, *J. Atmos. Solar Terr. Phys.*, **59**, 371, 1997a

Hines, C. O., Doppler-spread parameterization of gravity-wave momentum deposition in the middle atmosphere, 2, Broad and quasi monochromatic spectra, and implementation, *J. Atmos. Solar Terr. Phys.*, **59**, 387, 1997b

Holton, J. R., and W. M. Wehrbein, The role of forced planetary waves in the annual cycle of the zonal mean circulation of the middle atmosphere, , *J. Atmos. Sci.*, **38**, 1504, 1981

Holton, J. R., The generation of mesospheric planetary waves by zonally asymmetric gravity wave breaking, *J. Atmos. Sci.*, **41**, 3427, 1984

Lindzen R. S., Turbulence and stress due to gravity wave and tidal breakdown, *J. Geophys., Res.*, **86**, 9707, 1981

Mayr, H. G., J. G. Mengel, C. A. Reddy, K. L. Chan, and H. S. Porter, The role of gravity waves in maintaining the QBO and SAO at equatorial latitudes, *Advances in Space Research*, **24**, 1541, 1999

Mayr, H. G., J. G. Mengel, K. L. Chan, and H. S. Porter, Seasonal variations of the diurnal tide induced by gravity wave filtering, *Geophys. Res. Lett.*, **25**, 943, 1998

Meek, C. E., et al., Global study of northern hemisphere quasi 2-day wave events in recent summers near 90 km altitude, *J. Atm. Terr. Phys.*, **58**, 1401, 1996

Muller, H. G., and L. Nelson, A traveling quasi 2-day wave in the meteor region, *J. Atm. Terr. Phys.*, **40**, 761, 1978

Norton, W. A., and J. Thuburn, The two-day wave in a middle atmosphere GCM, *Geophys. Res. Lett.*, **23**, 2113, 1996

Norton, W. A., and J. Thuburn, Sensitivity of mesospheric mean flow, planetary waves and tides to strength of gravity wave drag, J. *Geophys. Res.*, **104**, 30,897, 1999

Phillips, A., Simultaneous observations of the quasi 2-day wave at Manson, Antarctica, and Adelaide, South Australia, *J. Atm. Terr. Phys.*, **51**, 761, 1989

Plumb, R. A., Baroclinic instability of the summer mesosphere: A mechanism for the quasi-2-day wave?, *J. Atmos. Sci.*, **40**, 262, 1983

Plumb, R. A., R. A. Vincent, and R. L. Craig, The quasi-2-day wave event of January 1984 and its impact on the mean mesospheric circulation, *J. Atmos. Sci.*, **44**, 3030, 1987

Poole, L. M. G., The characteristics of mesospheric two-day wave as observed at Grahamstown (33.3°S, 26.5°E), *J. Atm. Terr. Phys.*, **52**, 259, 1990

Shepherd, G. G., et al., WINDII, the Wind Imager Interferometer on the Upper Atmosphere Research Satellite, *J. Geophys. Res.*, **98**, 10,7725, 1993

Smith, A., K., Longitudinal variations in mesospheric winds: Evidence for gravity wave filtering by planetary waves, *J. Atmos. Sci.*, **53**, 1156, 1996

Smith, A., K., Stationary planetary waves in upper mesospheric winds, *J. Atmos. Sci.*, **54**, 2129, 1997

Tsuda, T., S. Kato, and R. A. Vincent, Long period oscillations observed by the Kyoto meteor radar and comparison of the quasi 2-day wave with Adelaide MF radar observations, *J. Atm. Terr. Phys.*, **50**, 225, 1988

Volland, H., *Atmospheric Tidal and Planetary Waves*, Kluwer Academic Publ., Boston, MA, 1988

Wang, D. W., W. E. Ward, G. G. Shepherd, and D. L. Wu, Stationary planetary waves inferred from WINDII wind data taken within altitudes 90-120 km during 1991-96, *J. Atmos. Sci.*, **57**, 1906, 2000

Williams, P. J., N. J. Mitchell, A. G. Beard, V. S. Howells, and H. G. Muller, The coupling of planetary waves, tides, and gravity waves in the mesosphere and lower thermosphere, *Adv. Space Res.*, **24**, 1571, 1999

Wu, D. L., P. B. Hays, W. R. Skinner et al., Observations of the quasi 2-day wave from the High Resolution Doppler Imager on UARS, *Geophys. Res. Lett.*, **20**, 2853, 1993

Zhou, Q. H., Radar observations of longitudinal variability of tidal/planetary waves and mean motions in the tropical mesosphere, *J. Geophys. Res.*, **105**, 2151, 2000

Zhu, X, Radiative cooling calculated by random band models with S-1-beta tailed distribution, *J. Atmos. Sci.*, **46**, 511, 1989

Figure Captions

Figure 1a. Time series describing the seasonal variations of the zonal winds in the planetary waves (PW) for m = 1 at 48° N and at different altitudes from 40 to 100 km, computed with gravity wave (GW) forcing and with the zonal mean (m = 0) temperature and wind fields as input. The PW are generated in the model purely by dynamical interactions without external time dependent energy or momentum sources. The PW amplitudes at 40 km are negligibly small, grow from 60 to 80 km, and are attenuated at 100 km. Short-period (about 4 days) monochromatic waves are generated in summer and winter, long period waves around spring and fall seasons.

Figure 1b. Same as Figure 1a but computed without GW forcing and with the zonal mean (m = 0) temperature and wind fields as input. Note that PW's are generated in summer, winter, and fall seasons, in part due to baroclinic instability (driven in turn by GW's). But the amplitudes are much smaller than those in Figure 1a, when GW are directly involved in amplifying the waves

Figure 2. Zonal winds at 80 km for PW's (computed with GW forcing as in Figure 1a) with m = 1 plotted versus latitude and time following June solstice. Note that the oscillating winds are larger in summer than in winter and grow in magnitude towards the poles. Initially at least the PW appear to propagate equatorward in the summer hemisphere.

Figure 3. Zonal winds at polar latitudes in the summer hemisphere for PW's (computed with GW forcing as in Figure 1a) with m = 1 plotted versus height and time following June solstice. The vertical wavelengths are large, characteristic of the PW's computed in the model, which indicates that the waves are not propagating freely but are generated throughout the mesosphere.

Figure 4. (a) Time segment (2 months) of zonal wind oscillations (computed with GW forcing as in Figure 1a) for m = 1 at 80 km and 48° N in summer following June solstice, and amplitude spectra of the largest waves (in the time segment), propagating eastward and westward. Note that the dominant PW's with a period of about 4 days propagates westward. (b) Same as (a) but for the winter season, where the waves propagate primarily eastward with periods between 3 and 10 days.

Figure 5. (a) Same as Figure 1a but for m = 2. Without GW source (b), the computed PW's are again much weaker, similar to those shown in Figure 1b.

Figure 6. Same as Figure 2 but for m = 2. Here there is some indication that the PW's propagate poleward from mid latitudes.

Figure 7. Same as Figure 3 but for m = 3. Again, the vertical wavelengths are large, indicating that the waves are not propagating freely but are excited throughout the region.

Figure 8. Zonal winds and amplitude spectra like in Figure 4 but for m = 2. The peak amplitudes occur at periods around 2.5 and 3.5 days respectively for the westward and eastward propagating waves during the summer (a) and winter (b) months respectively.

Figure 9a. Same as Figure 1a but for meridional winds at the equator and for m = 3.

Figure 9b. Same as Figure 9a but without GW momentum source.

Figure 10. Same as Figure 2 but for meridional winds and m = 3. The PW's have large meridional winds at equatorial latitudes, like Rossby gravity waves, and tend to propagate to higher latitudes in the summer hemisphere.

Figure 11. Same as Figure 3 but for meridional winds and m = 3. Note the large vertical wavelengths and downward phase progression at heights above 65 km. Below that altitude, the phase progresses upwards indicating that waves propagate down.

Figure 12. Zonal winds and amplitude spectra like in Figure 4 but for m = 3. The peak amplitudes occur at periods near 2 days for the westward and eastward propagating waves during the summer (a) and winter (b) months respectively.

Figure 13. Snapshot of horizontal wind vectors (computed with GW forcing as in Figure 1a) for m = 3 at 80 km plotted versus latitude and longitude during a period near June solstice. Note the cells circling around the equator where the meridional winds are large but the zonal winds are small, characteristic of Rossby gravity waves.

Figure 14. Same as Figure 9a but for m = 4. Without GW source, the computed PW's (not shown) are again much weaker, similar to those shown in Figure 9b.

Figure 15. Same as Figure 10 but for m = 4.

Figure 16. Zonal winds and amplitude spectra like in Figure 12 but for m = 4. Again, the peak amplitudes occur at periods near 2 days for the westward and eastward propagating waves during the summer (a) and winter (b) months respectively.

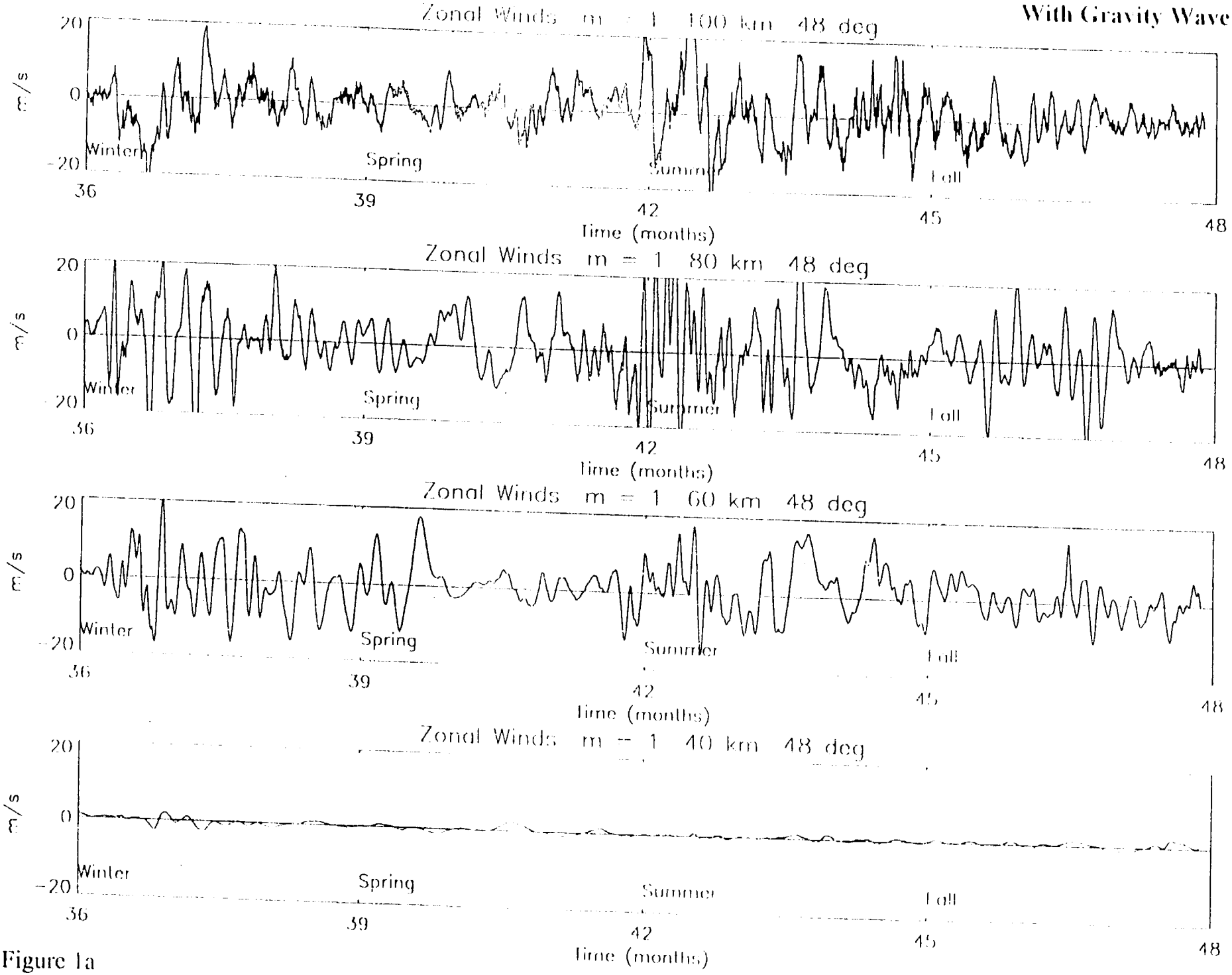
Zonal Winds m = 1 100 km 48 deg
m/s
20
0
-20
Winter
Spring
Summer
Fall
36
39
42
45
48
Time (months)
Zonal Winds m = 1 80 km 48 deg
m/s
20
0
-20
Winter
Spring
Summer
Fall
36
39
42
45
48
Time (months)
Zonal Winds m = 1 60 km 48 deg
m/s
20
0
-20
Winter
Spring
Summer
Fall
36
39
42
45
48
Time (months)
Zonal Winds m = 1 40 km 48 deg
m/s
20
0
-20
Winter
Spring
Summer
Fall
36
39
42
45
48
Time (months)

Figure 1a

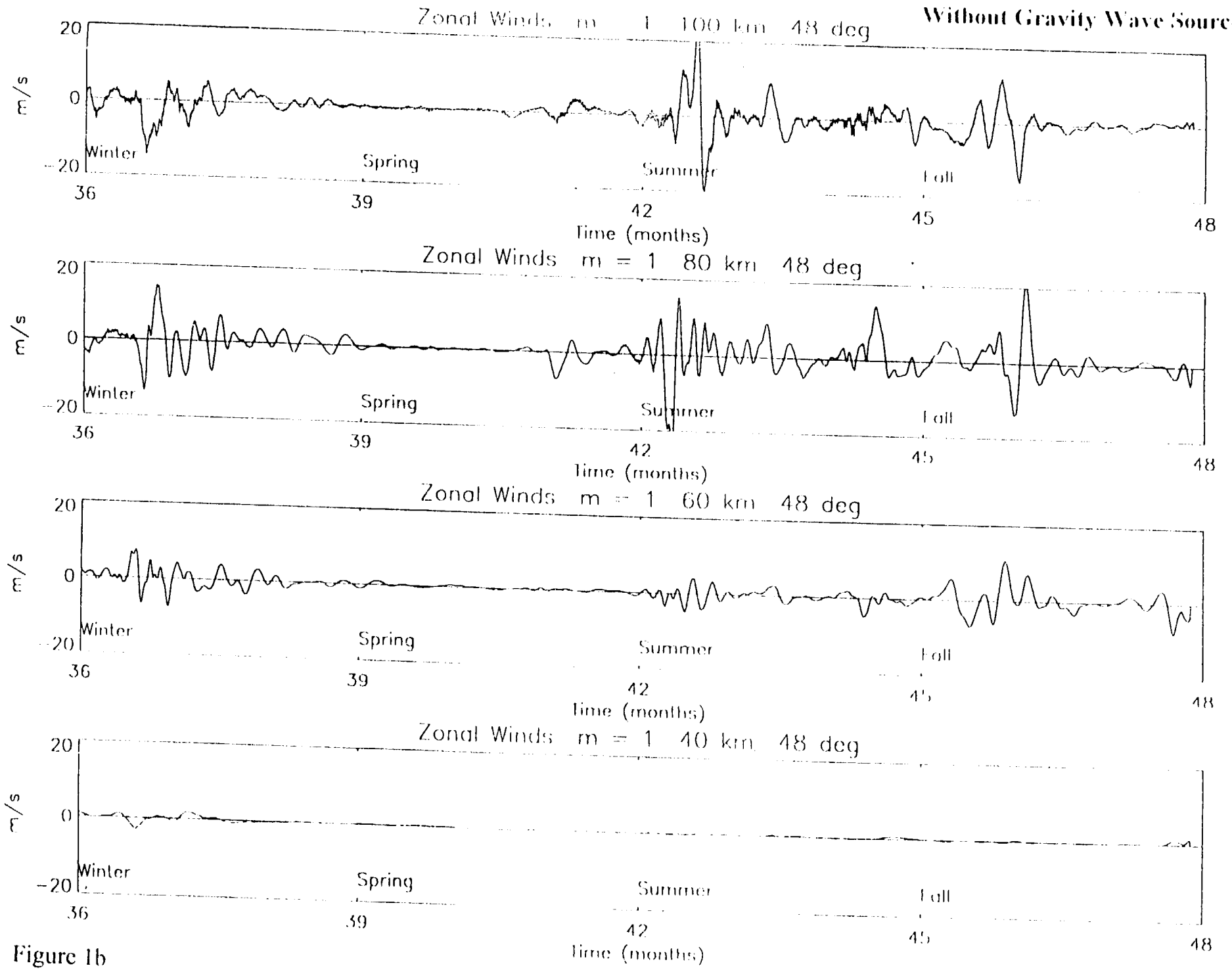
Without Gravity Wave Source
Zonal Winds m = 1 100 km 48 deg
Zonal Winds m = 1 80 km 48 deg
Zonal Winds m = 1 60 km 48 deg
Zonal Winds m = 1 40 km 48 deg
m/s
20
0
-20
Winter
Spring
Summer
Fall
36
39
42
45
48
Time (months)

Figure 1b

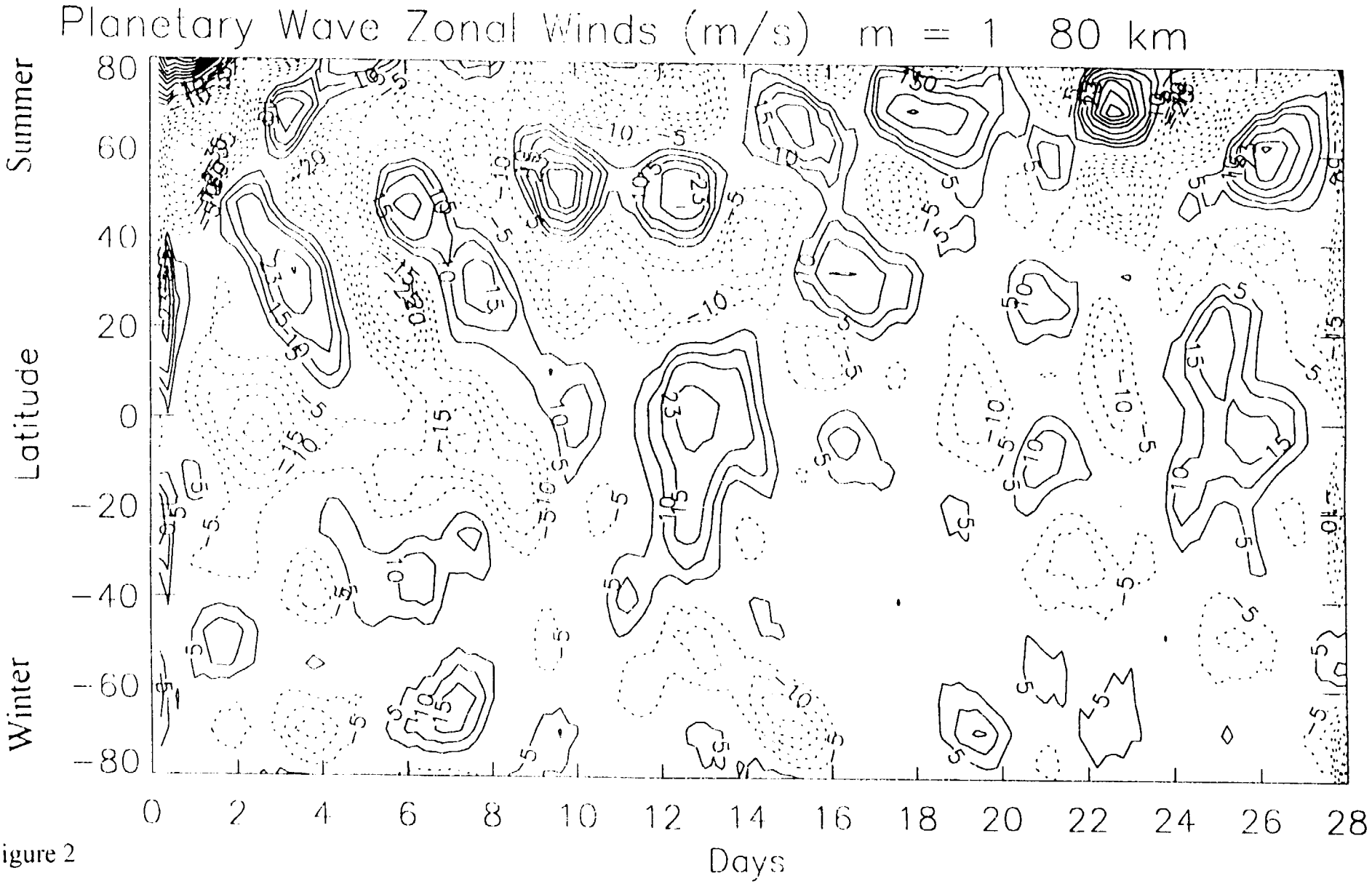
Planetary Wave Zonal Winds (m/s) m = 1 80 km
Summer
Latitude
Winter
80
60
40
20
0
−20
−40
−60
−80
0
2
4
6
8
10
12
14
16
18
20
22
24
26
28
Days

Figure 2

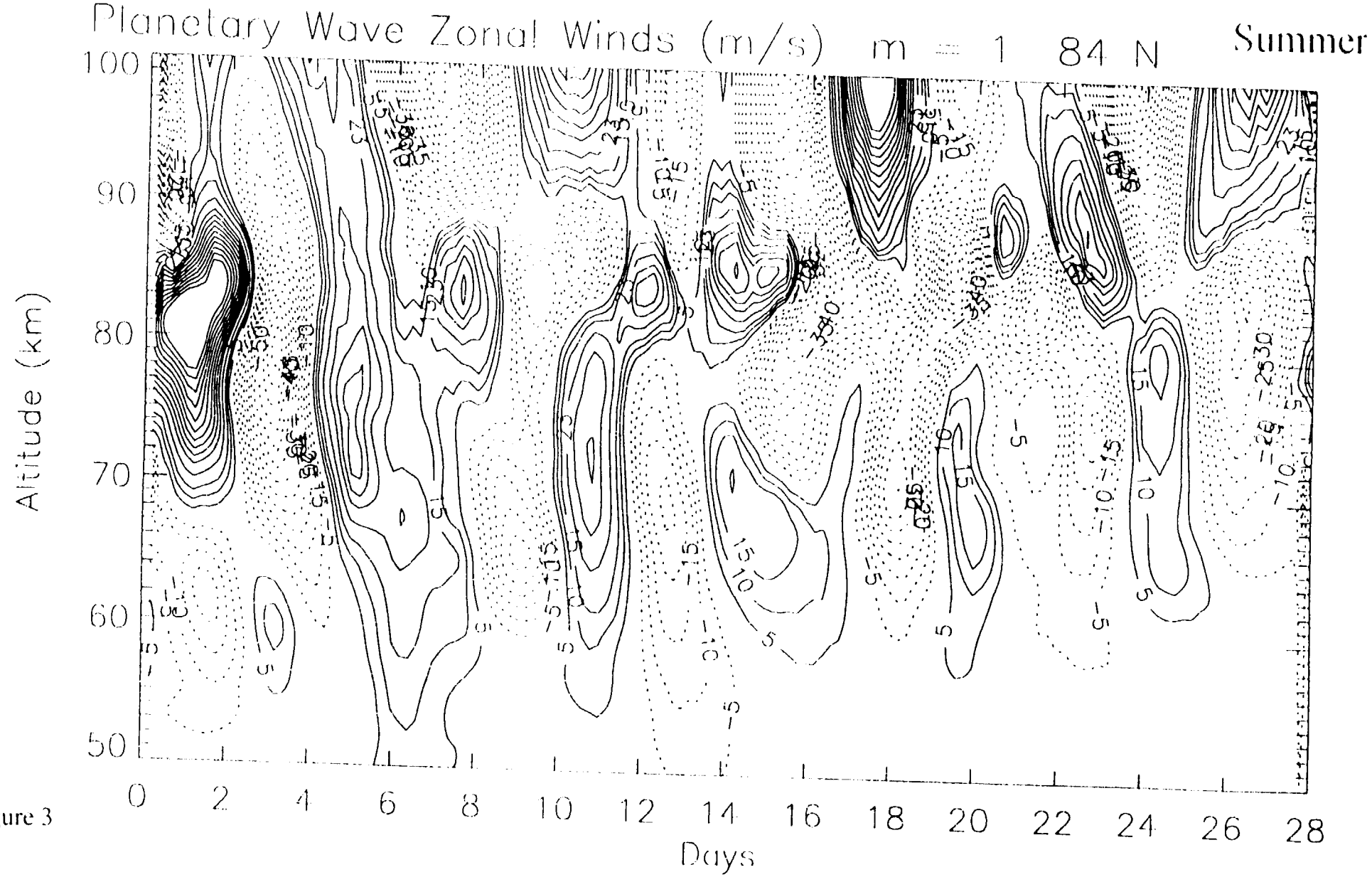
Planetary Wave Zonal Winds (m/s) m = 1 84 N
Summer
Altitude (km)
100
90
80
70
60
50
0
2
4
6
8
10
12
14
16
18
20
22
24
26
28
Days

Figure 3

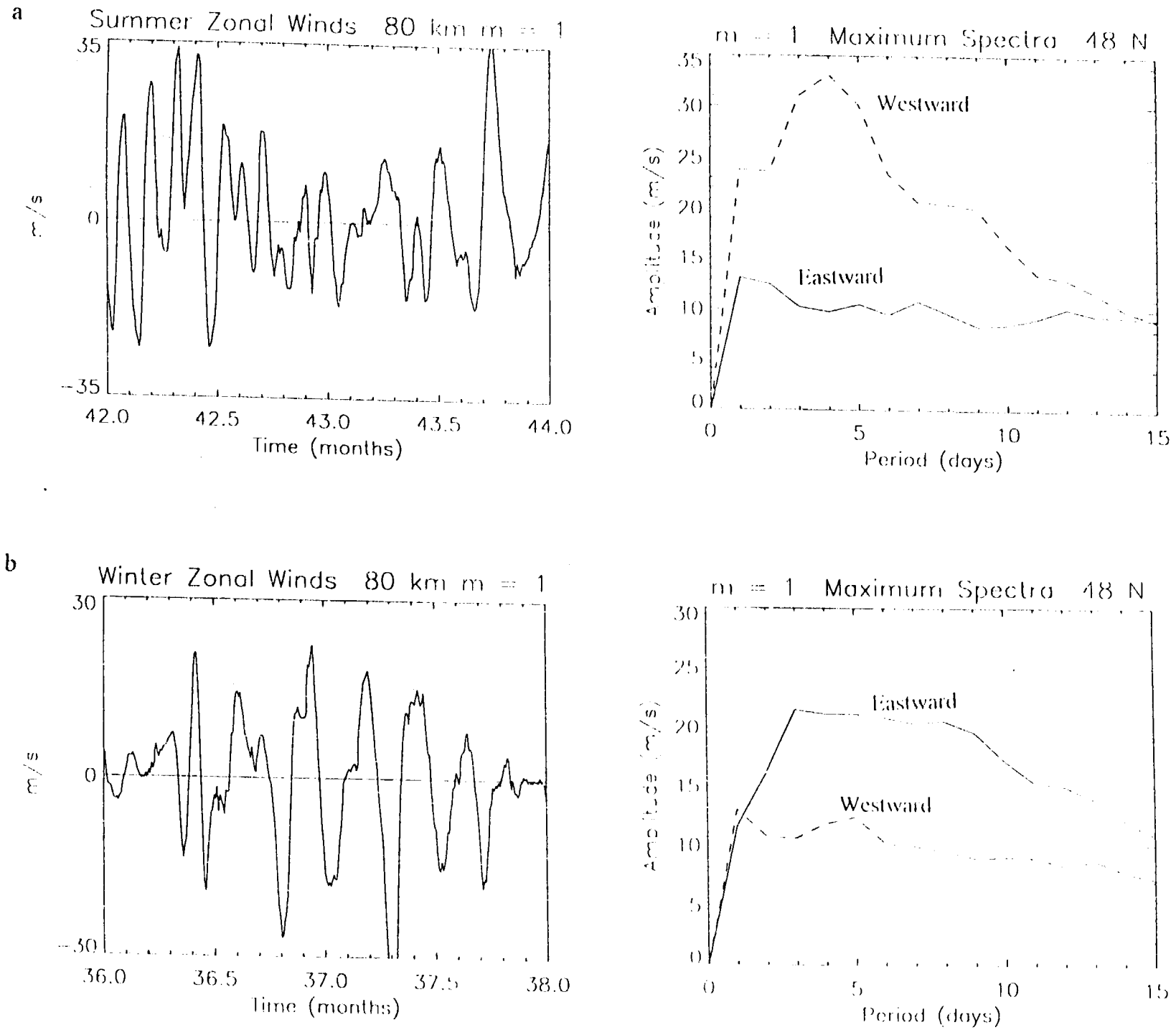
a
Summer Zonal Winds 80 km m = 1
35
0
-35
m/s
42.0
42.5
43.0
43.5
44.0
Time (months)
m = 1 Maximum Spectra 48 N
Westward
Eastward
Amplitude (m/s)
0
5
10
15
20
25
30
35
0
5
10
15
Period (days)
b
Winter Zonal Winds 80 km m = 1
30
0
-30
m/s
36.0
36.5
37.0
37.5
38.0
Time (months)
m = 1 Maximum Spectra 48 N
Eastward
Westward
Amplitude (m/s)
0
5
10
15
20
25
30
0
5
10
15
Period (days)

Figure 4

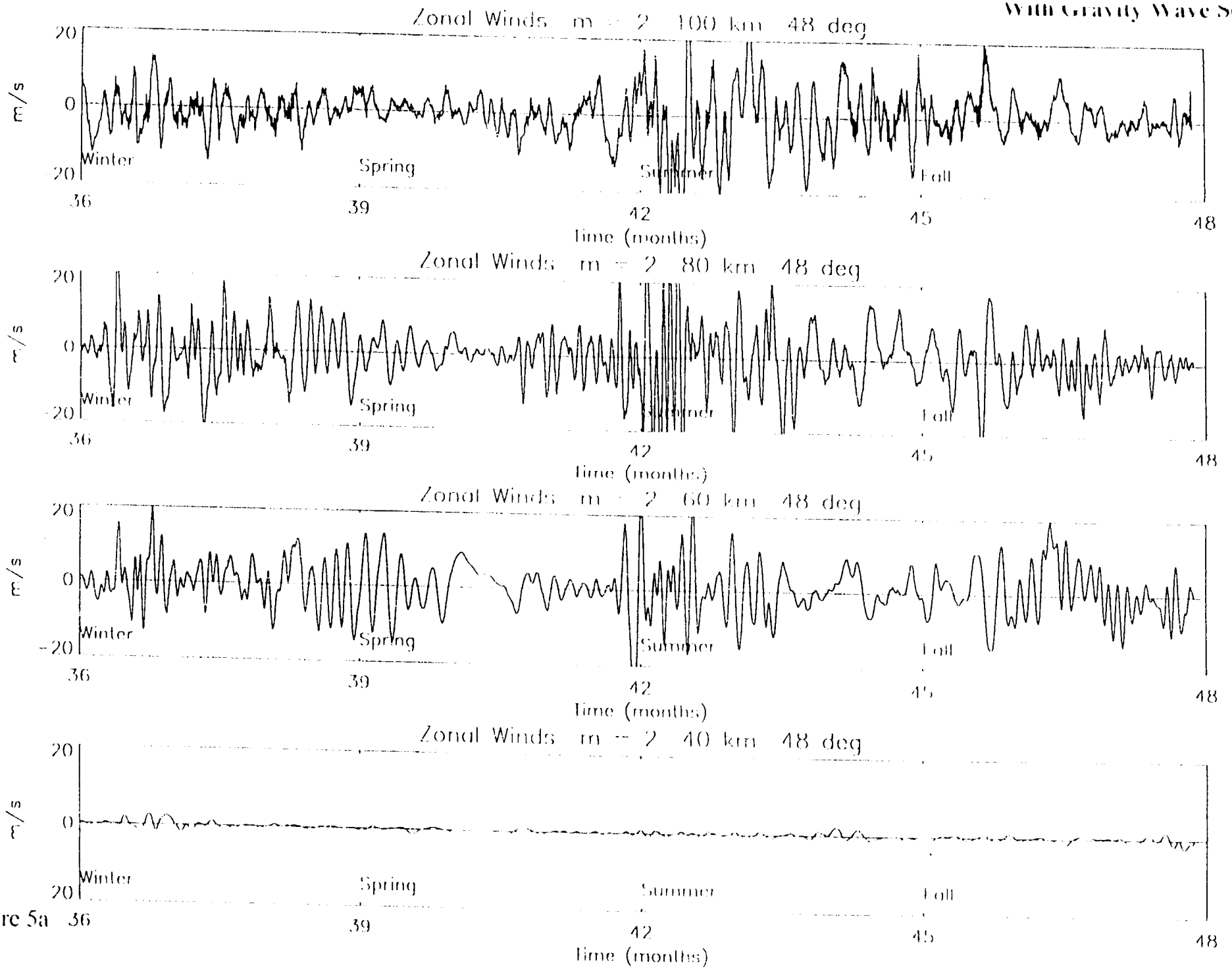
Zonal Winds m = 2 100 km 48 deg
Zonal Winds m = 2 80 km 48 deg
Zonal Winds m = 2 60 km 48 deg
Zonal Winds m = 2 40 km 48 deg
m/s
20
0
-20
Winter
Spring
Summer
Fall
36
39
42
45
48
Time (months)

Figure 5a

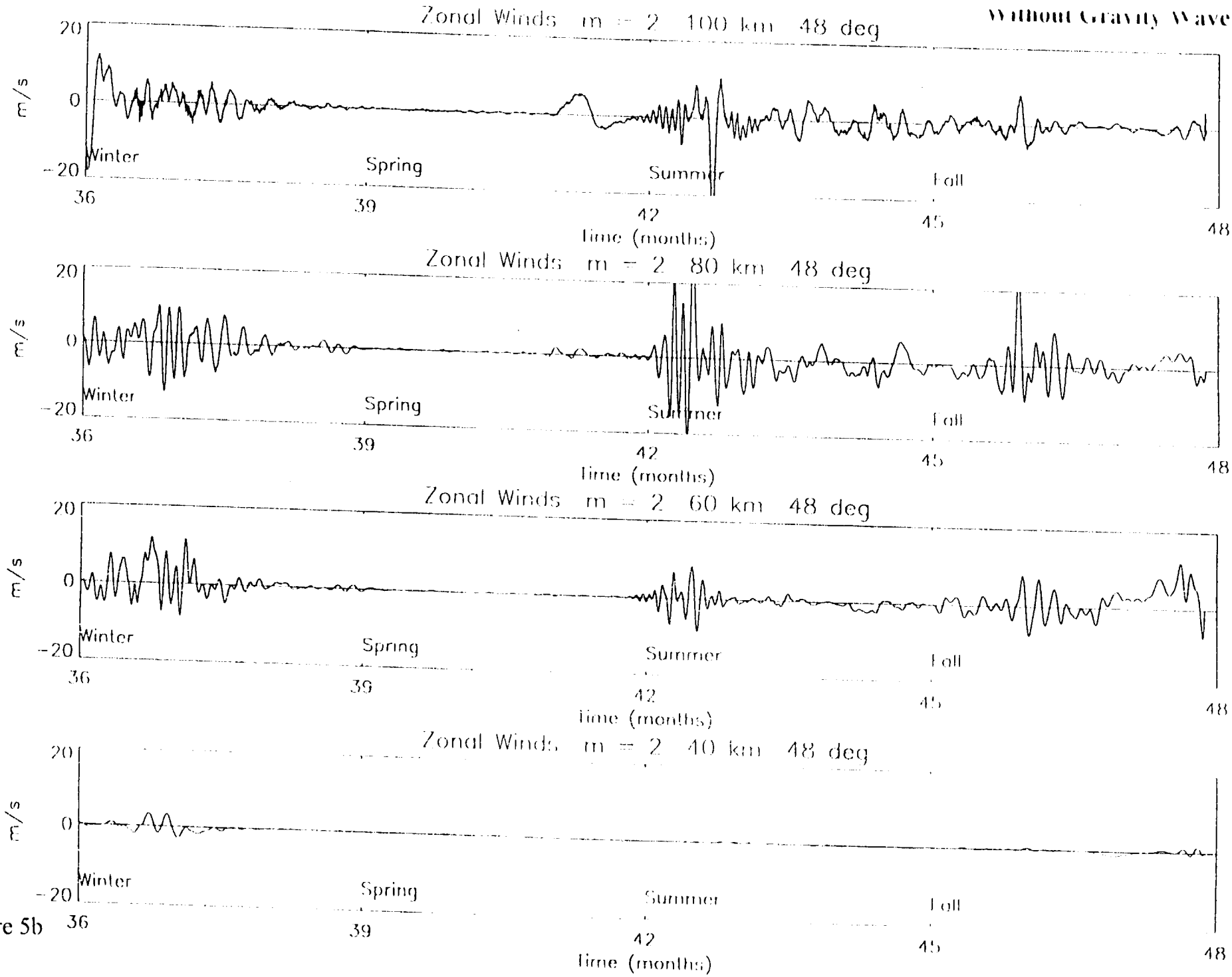
Zonal Winds m = 2 100 km 48 deg
Zonal Winds m = 2 80 km 48 deg
Zonal Winds m = 2 60 km 48 deg
Zonal Winds m = 2 40 km 48 deg
m/s
20
0
-20
Winter
Spring
Summer
Fall
36
39
42
45
48
Time (months)

Figure 5b

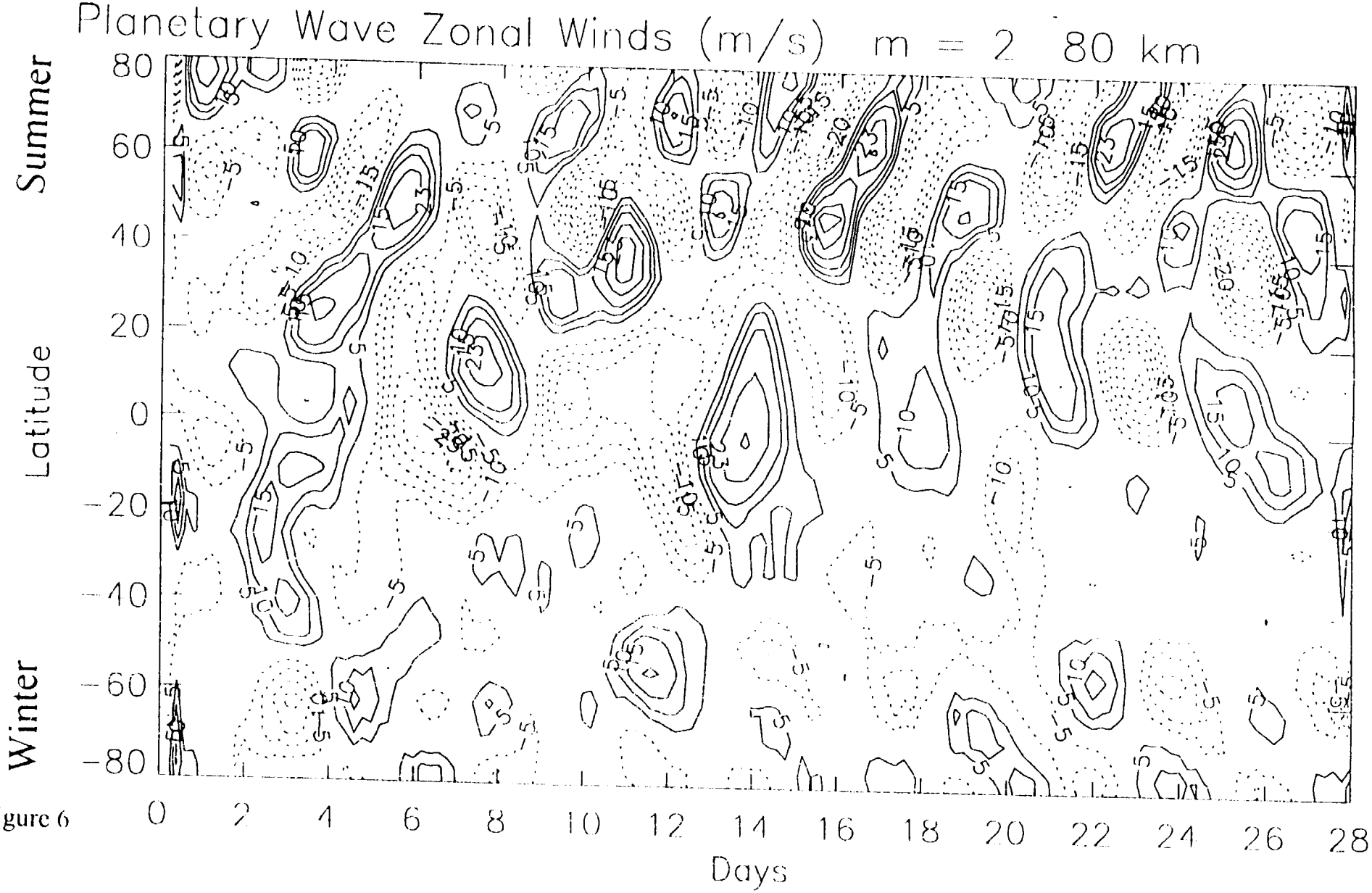
Planetary Wave Zonal Winds (m/s) m = 2 80 km
Summer
Winter
Latitude
80
60
40
20
0
-20
-40
-60
-80
0
2
4
6
8
10
12
14
16
18
20
22
24
26
28
Days

Figure 6

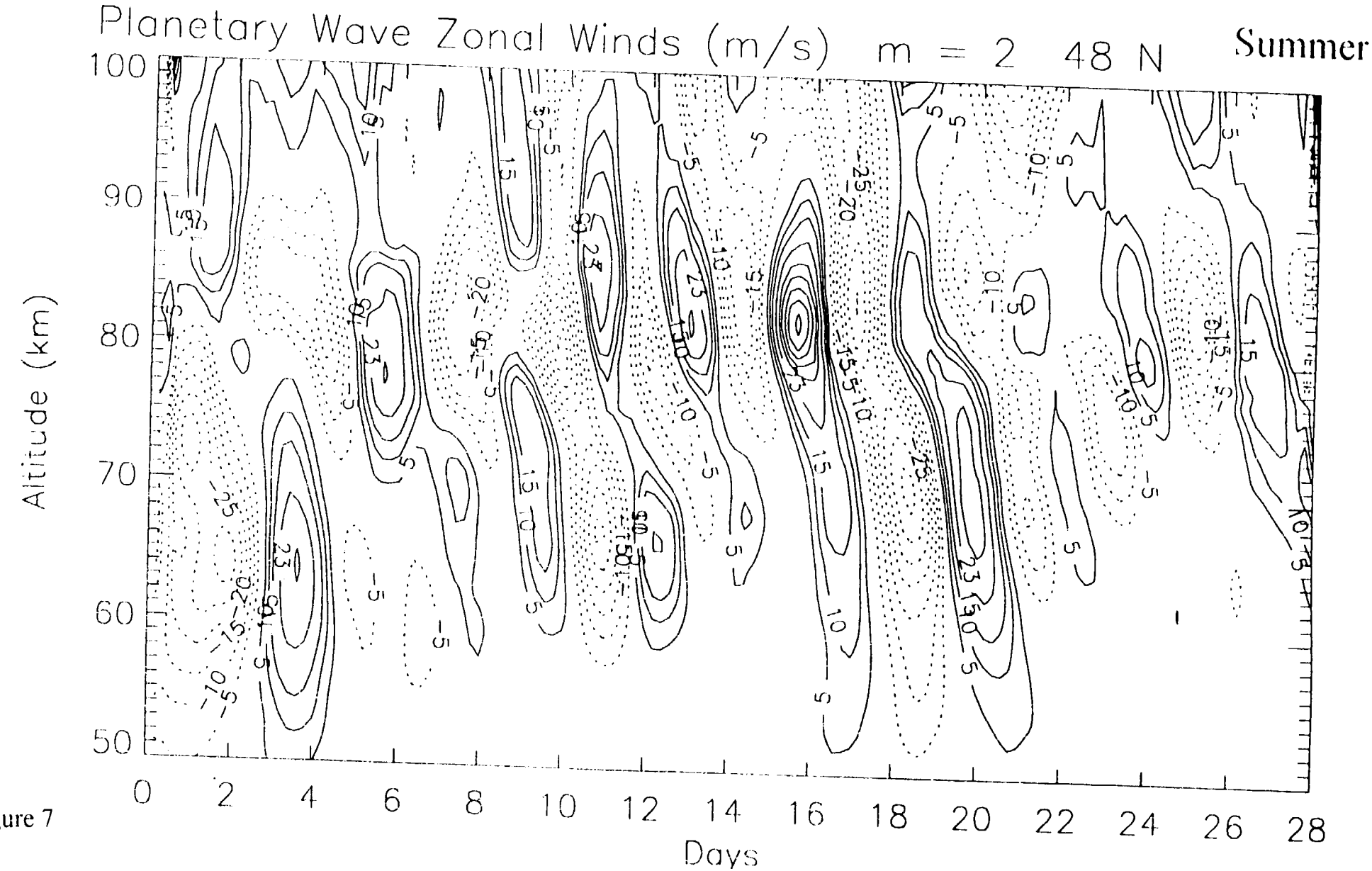
Planetary Wave Zonal Winds (m/s) m = 2 48 N
Summer
Altitude (km)
100
90
80
70
60
50
0
2
4
6
8
10
12
14
16
18
20
22
24
26
28
Days

Figure 7

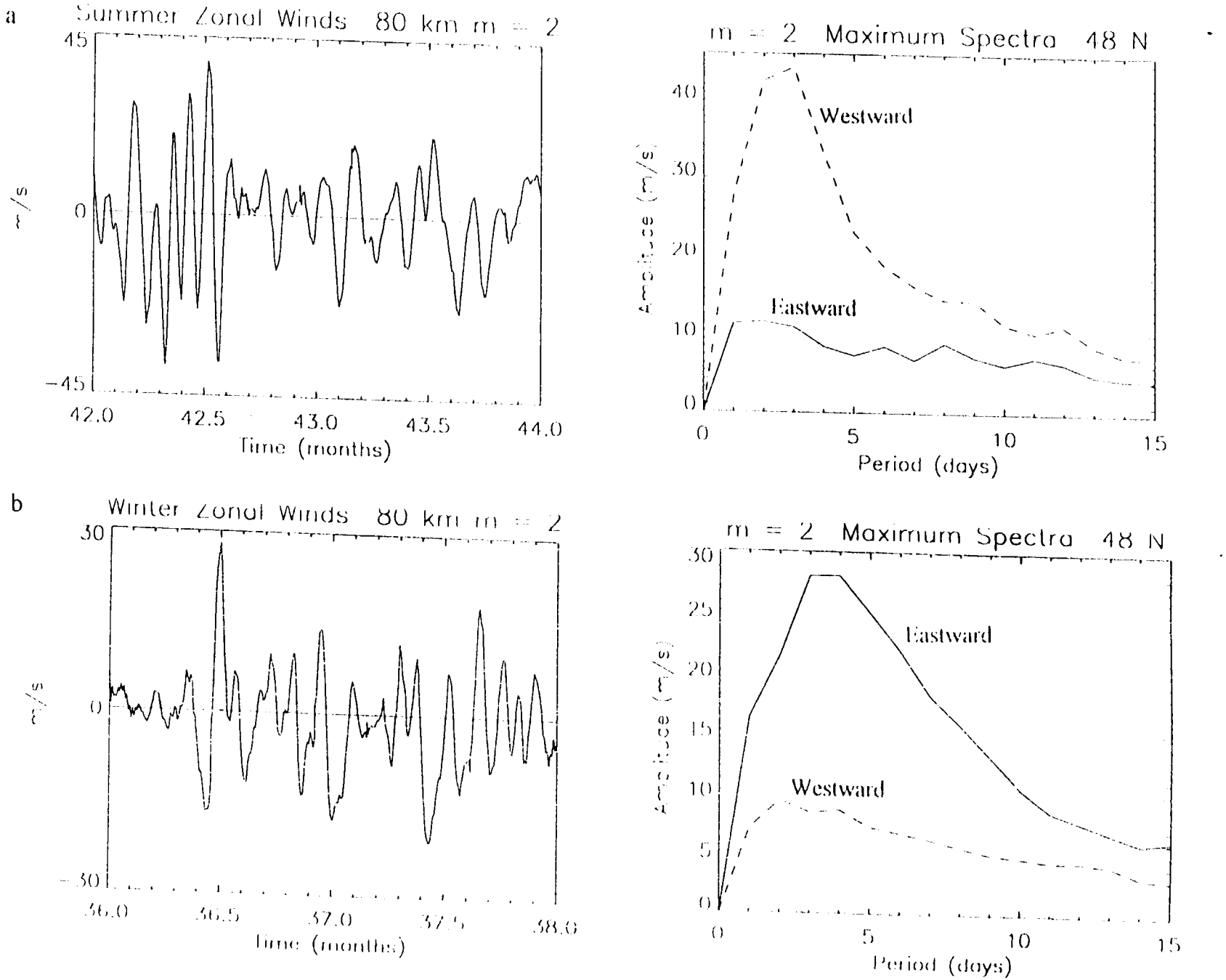
a
Summer Zonal Winds 80 km m = 2
45
0
−45
m/s
42.0
42.5
43.0
43.5
44.0
Time (months)
m = 2 Maximum Spectra 48 N
Westward
Eastward
Amplitude (m/s)
40
30
20
10
0
0
5
10
15
Period (days)
b
Winter Zonal Winds 80 km m = 2
30
0
−30
m/s
36.0
36.5
37.0
37.5
38.0
Time (months)
m = 2 Maximum Spectra 48 N
Eastward
Westward
Amplitude (m/s)
30
25
20
15
10
5
0
0
5
10
15
Period (days)

Figure 8

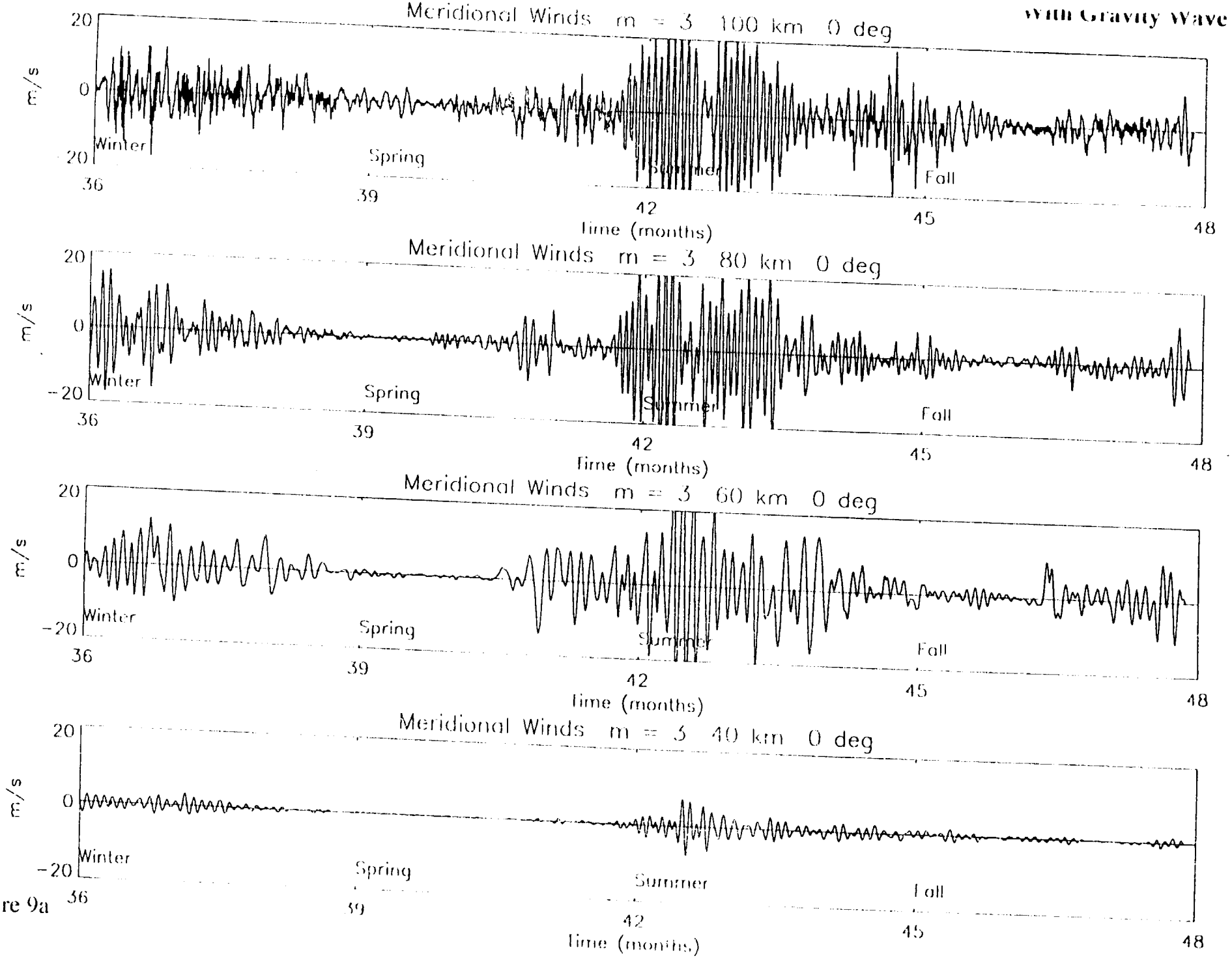
Meridional Winds m = 3 100 km 0 deg
m/s
20
0
-20
Winter
Spring
Summer
Fall
36
39
42
45
48
Time (months)
Meridional Winds m = 3 80 km 0 deg
m/s
20
0
-20
Winter
Spring
Summer
Fall
36
39
42
45
48
Time (months)
Meridional Winds m = 3 60 km 0 deg
m/s
20
0
-20
Winter
Spring
Summer
Fall
36
39
42
45
48
Time (months)
Meridional Winds m = 3 40 km 0 deg
m/s
20
0
-20
Winter
Spring
Summer
Fall
36
39
42
45
48
Time (months)

Figure 9a

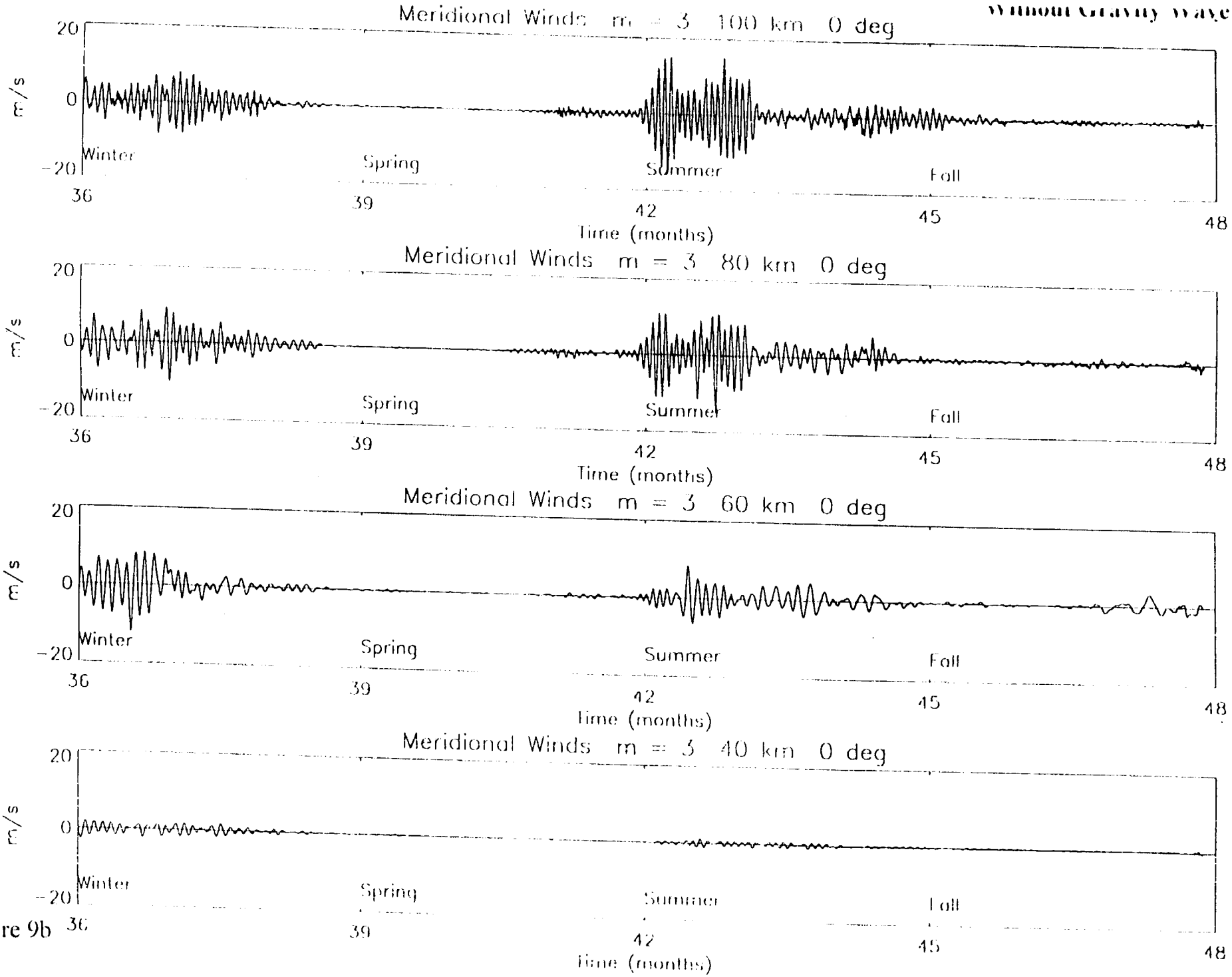
Meridional Winds m = 3 100 km 0 deg
Meridional Winds m = 3 80 km 0 deg
Meridional Winds m = 3 60 km 0 deg
Meridional Winds m = 3 40 km 0 deg
m/s
20
0
-20
Winter
Spring
Summer
Fall
36
39
42
45
48
Time (months)

Figure 9b

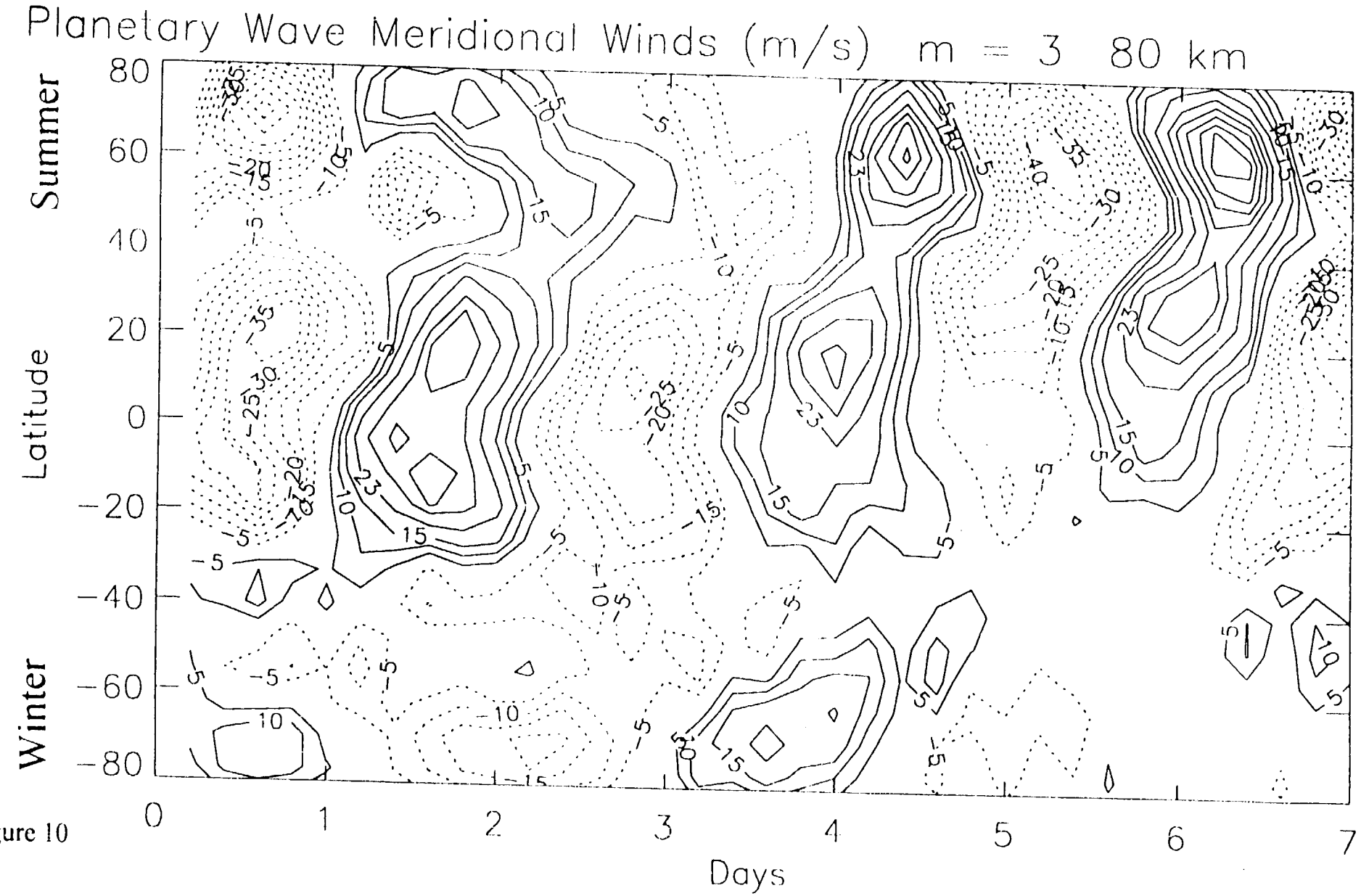
Planetary Wave Meridional Winds (m/s) m = 3 80 km
Summer
Winter
Latitude
80
60
40
20
0
-20
-40
-60
-80
0
1
2
3
4
5
6
7
Days

Figure 10

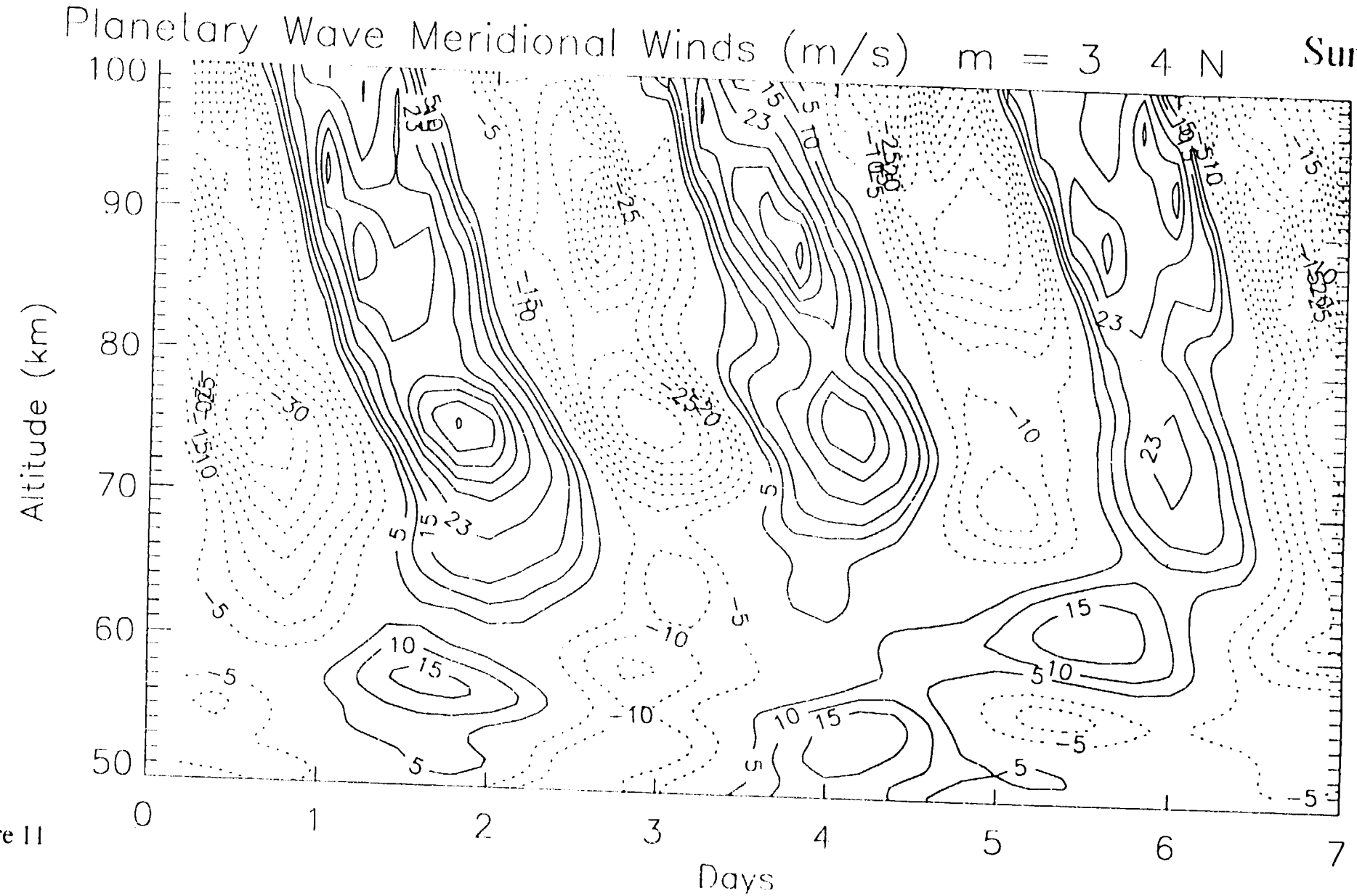
Planetary Wave Meridional Winds (m/s) m = 3 4 N
Summer
Altitude (km)
100
90
80
70
60
50
0
1
2
3
4
5
6
7
Days

Figure 11

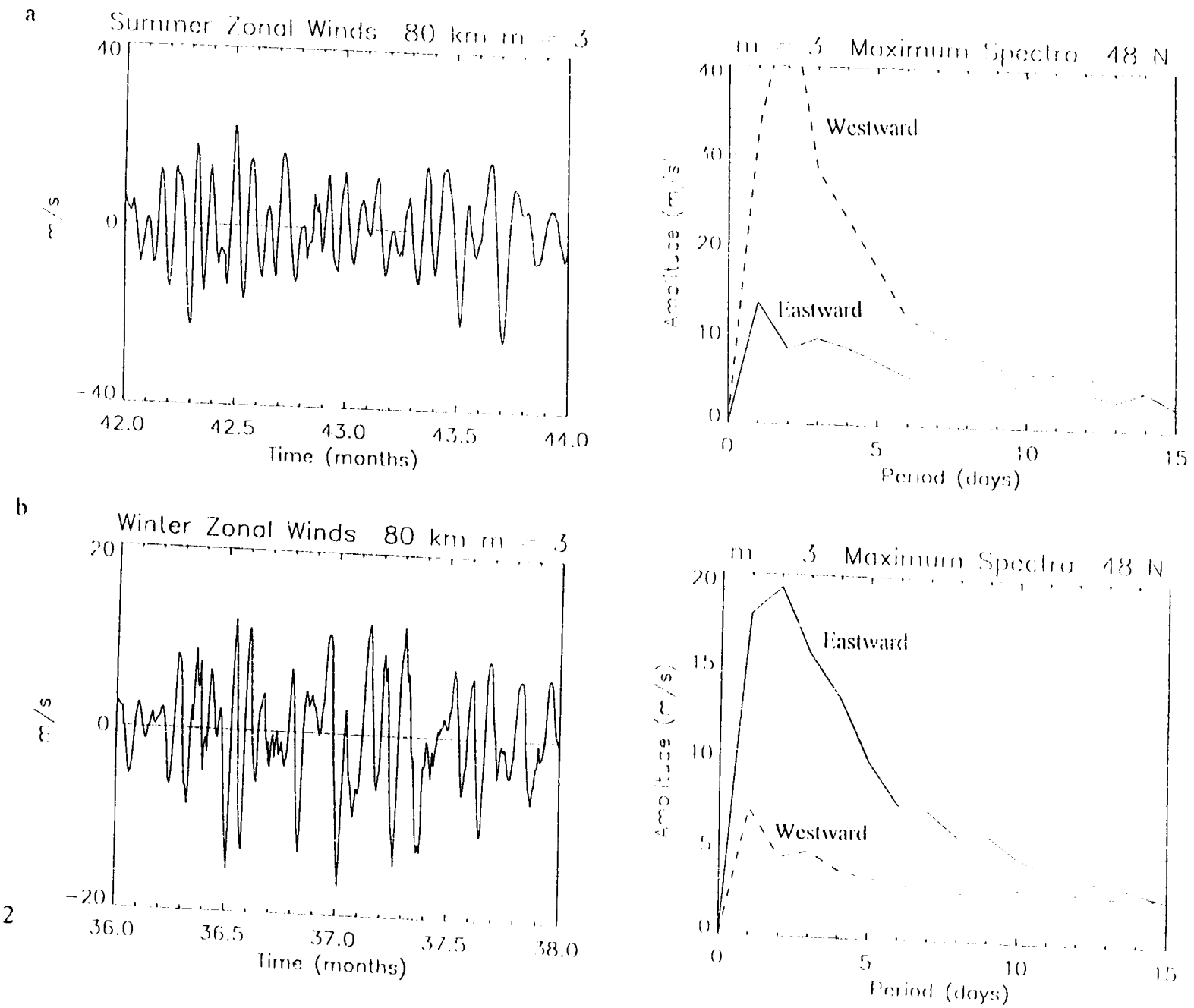
a
Summer Zonal Winds 80 km m = 3
40
0
-40
m/s
42.0
42.5
43.0
43.5
44.0
Time (months)
m = 3 Maximum Spectra 48 N
Westward
Eastward
Amplitude (m/s)
0
10
20
30
40
0
5
10
15
Period (days)
b
Winter Zonal Winds 80 km m = 3
20
0
-20
m/s
36.0
36.5
37.0
37.5
38.0
Time (months)
m = 3 Maximum Spectra 48 N
Eastward
Westward
Amplitude (m/s)
0
5
10
15
20
0
5
10
15
Period (days)

Figure 12

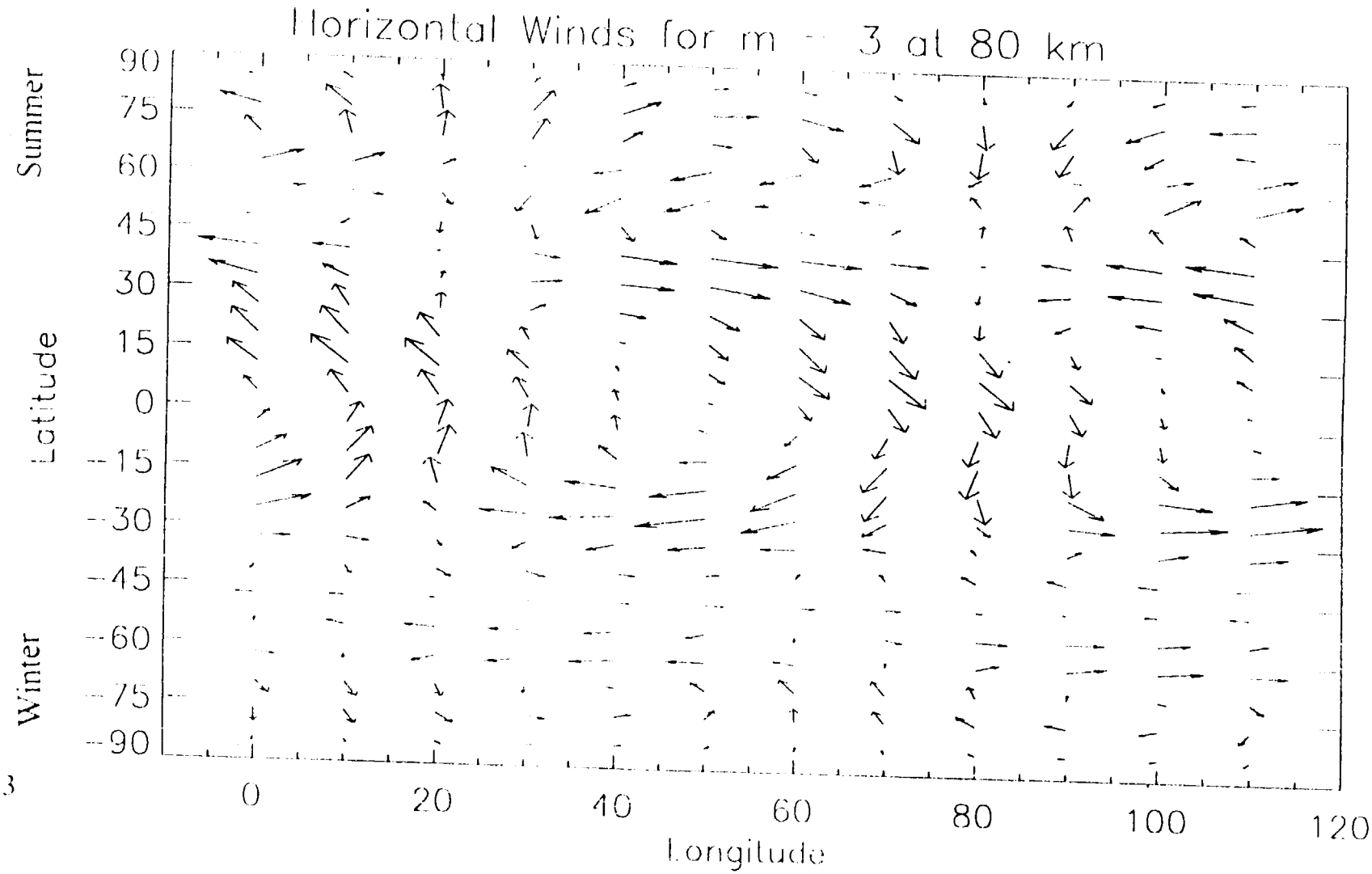
Horizontal Winds for m = 3 at 80 km
Summer
Winter
Latitude
90
75
60
45
30
15
0
-15
-30
-45
-60
-75
-90
0
20
40
60
80
100
120
Longitude

Figure 13

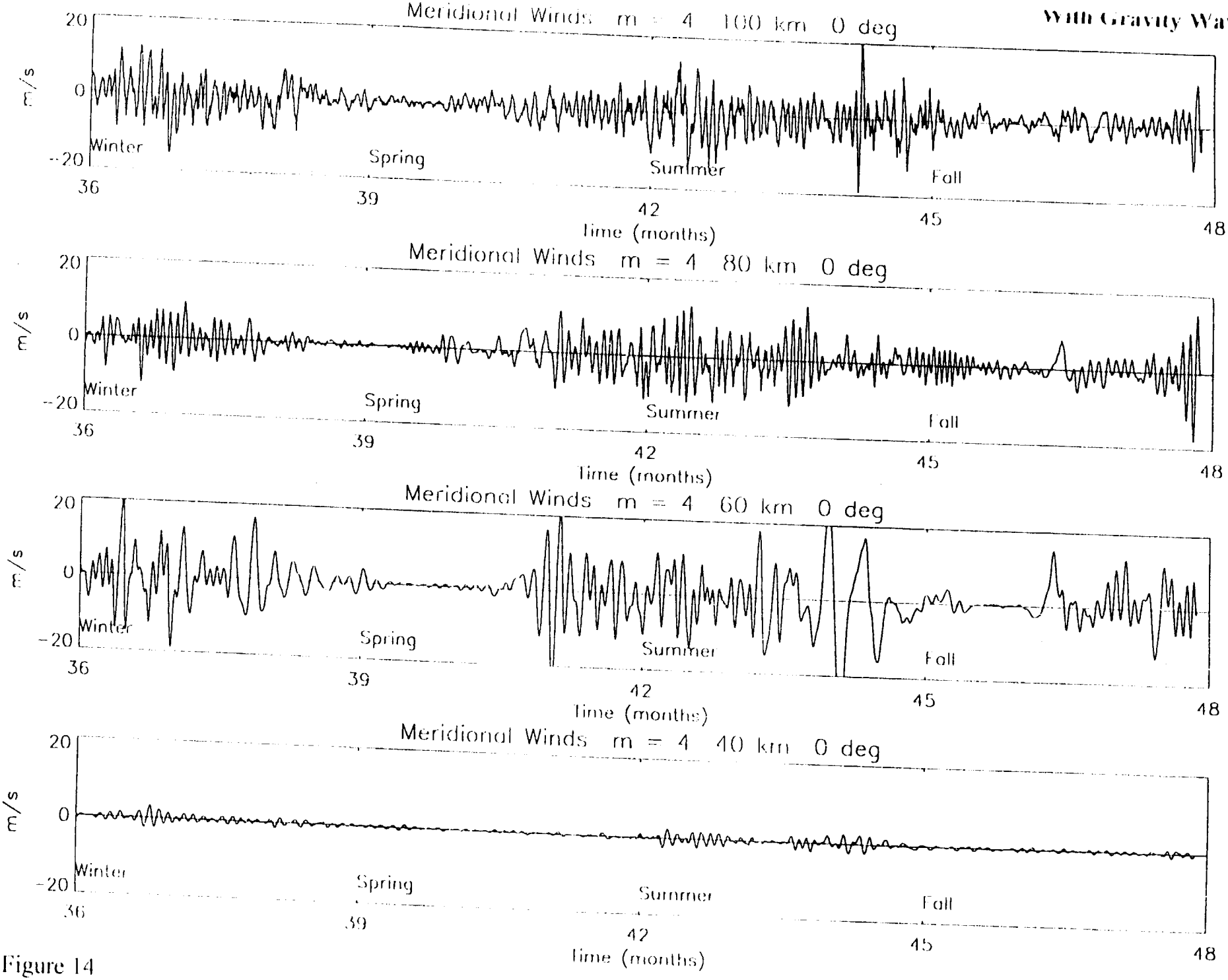
Meridional Winds m = 4 100 km 0 deg
20
0
-20
m/s
Winter
Spring
Summer
Fall
36
39
42
45
48
Time (months)
Meridional Winds m = 4 80 km 0 deg
20
0
-20
m/s
Winter
Spring
Summer
Fall
36
39
42
45
48
Time (months)
Meridional Winds m = 4 60 km 0 deg
20
0
-20
m/s
Winter
Spring
Summer
Fall
36
39
42
45
48
Time (months)
Meridional Winds m = 4 40 km 0 deg
20
0
-20
m/s
Winter
Spring
Summer
Fall
36
39
42
45
48
Time (months)

Figure 14

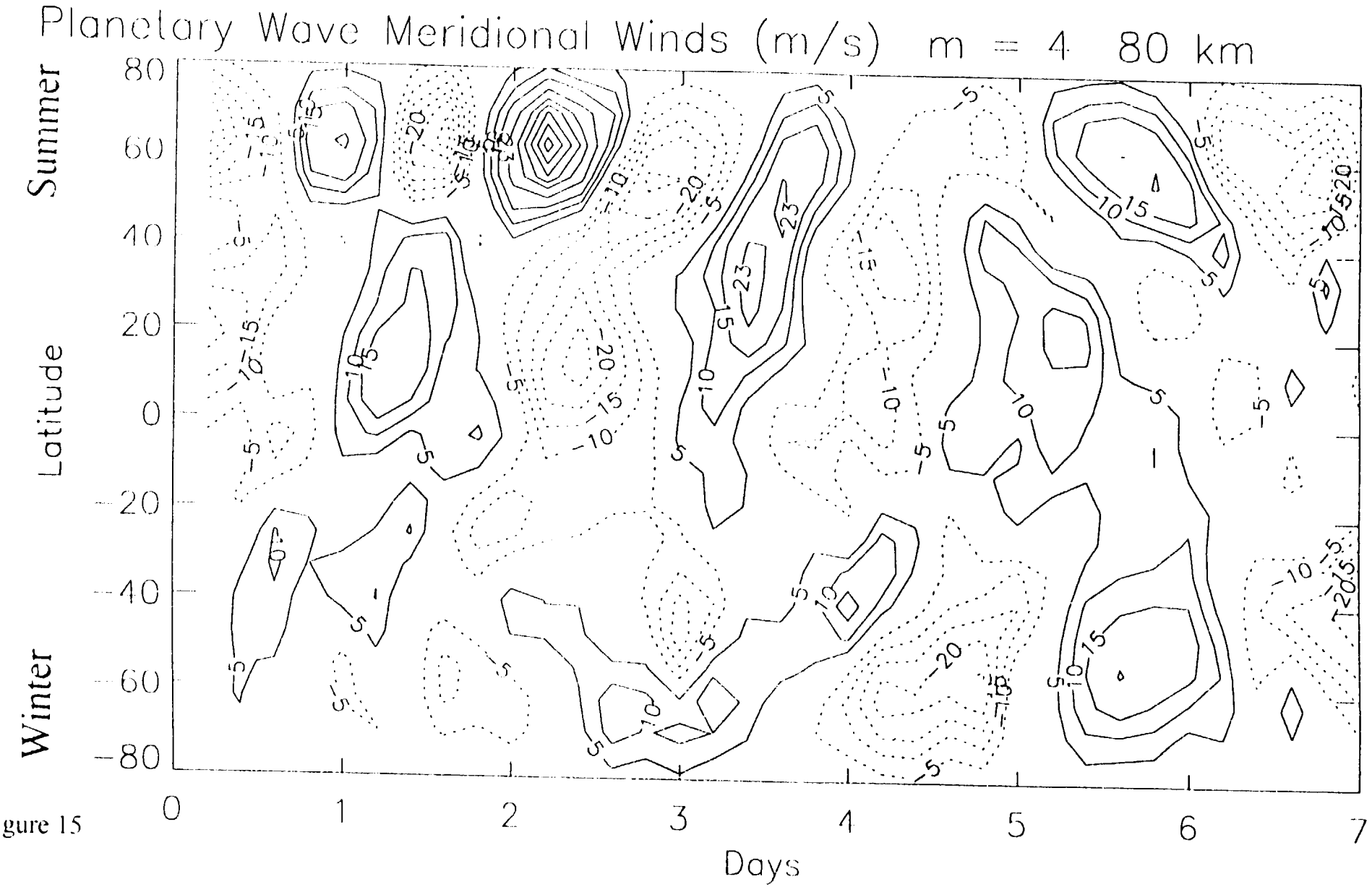
Planetary Wave Meridional Winds (m/s) m = 4 80 km
Summer
Latitude
Winter
80
60
40
20
0
-20
-40
-60
-80
0
1
2
3
4
5
6
7
Days

Figure 15

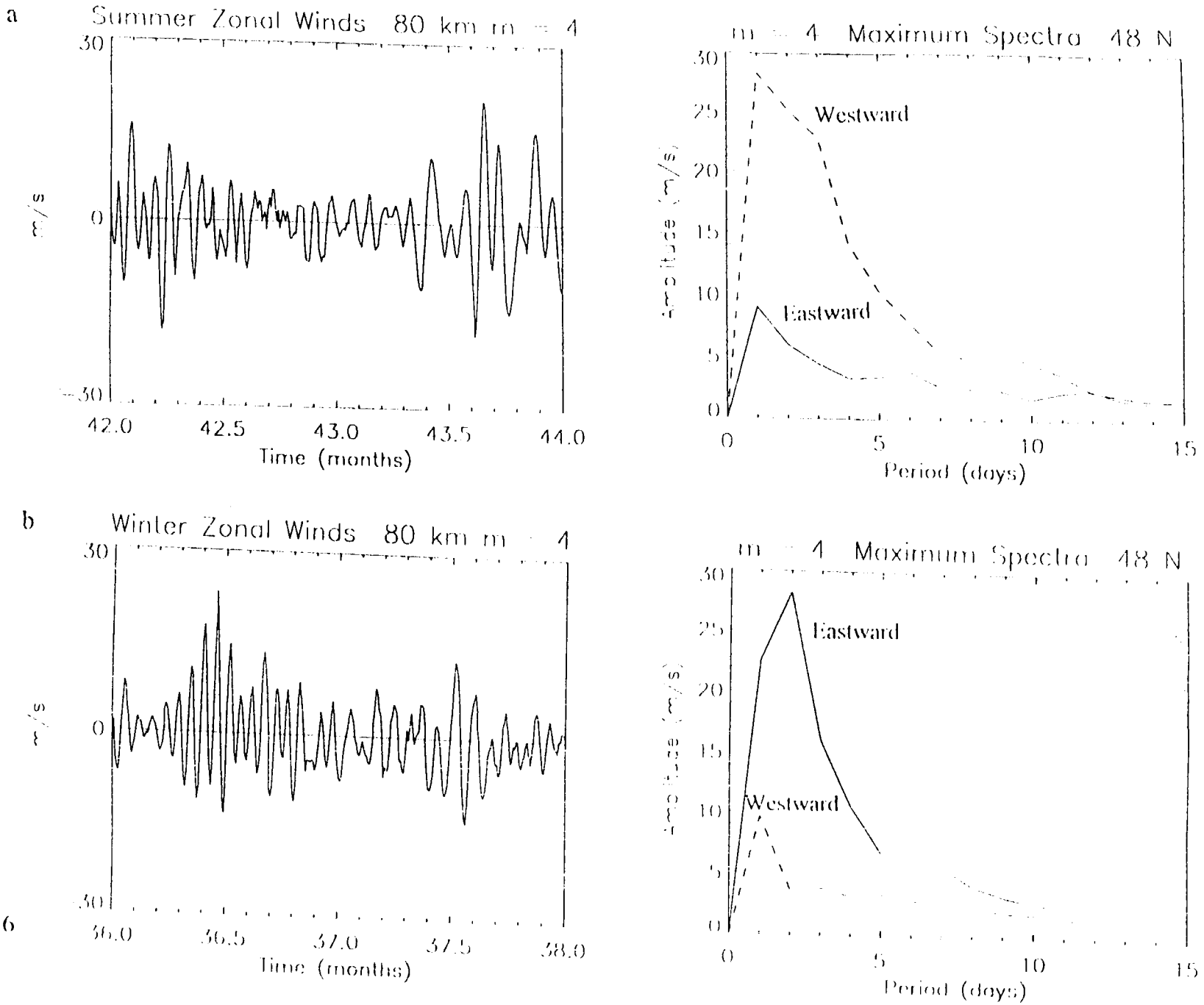
a
Summer Zonal Winds 80 km m = 4
30
0
-30
m/s
42.0
42.5
43.0
43.5
44.0
Time (months)
m = 4 Maximum Spectra 48 N
Westward
Eastward
Amplitude (m/s)
0
5
10
15
20
25
30
Period (days)
b
Winter Zonal Winds 80 km m = 4
30
0
-30
m/s
36.0
36.5
37.0
37.5
38.0
Time (months)
m = 4 Maximum Spectra 48 N
Eastward
Westward
Amplitude (m/s)
0
5
10
15
20
25
30
Period (days)

Figure 16